Published in final edited form as:
Nat Cell Biol. 2008 August ; 10(8): 979–986. doi:10.1038/ncb1758.

EphrinB1 Controls Cell-Cell Junctions through the Par Polarity Complex

Hyun-Shik Lee[1], **Tagvor G. Nishanian**[1], **Kathleen Mood**[1], **Yong-Sik Bong**[1,2], and **Ira O. Daar**[1]

1*Laboratory of Cell and Developmental Signaling, National Cancer Institute-Frederick, Frederick, Maryland 21702, USA.*

Abstract

A body of evidence is emerging that shows a requirement for ephrin ligands in the proper migration of cells, and the formation of cell and tissue boundaries. These processes are dependent upon the cell-cell adhesion system that plays a critical role in normal morphogenetic processes during development, as well as in invasion and metastasis[1–9]. Although ephrinB ligands are bi-directional signaling molecules, the precise mechanism by which ephrinB1 signals through its intracellular domain to regulate cell-cell adhesion in epithelial cells has remained elusive. Here, we present evidence that ephrinB1 associates with the Par polarity complex protein, Par-6, a scaffold protein required for establishing tight junctions, and can compete with the small GTPase Cdc42 for an association with Par-6. This competition results in inactivation of the Par complex, resulting in the loss of tight junctions. Moreover, the interaction between ephrinB1 and Par-6 is disrupted upon tyrosine phosphorylation of the intracellular domain of ephrinB1. Thus, we have identified a mechanism by which ephrinB1 signaling regulates cell-cell junctions in epithelial cells, and this may impact how we devise therapeutic interventions regarding these molecules in metastatic disease.

It has been known for over a decade that ephrinBs are bi-directional signaling molecules that can signal through their intracellular domains to regulate cell-cell boundaries and adhesion[10, 11]. EphrinB has been shown to interact with proteins that control cell migration through a G-protein coupled receptor[12], or by co-opting Dishevelled, a scaffold protein from the Wnt signaling pathway[13]. EphrinB can also regulate the actin cytoskeleton and cell morphogenesis via the adaptor protein Grb4/Nck2 and the G protein-coupled receptor kinase-interacting protein 1[14]. It has also been shown that gap junction communication may be regulated by ephrinB1 through an interaction with Connexin43[15]. Here, we provide mechanistic insight indicating that ephrinB1 regulates cell-cell junctions through the Par (partitioning defective) protein complex that has a central role in tight junction (TJ) formation, cell-cell adhesion, and cell polarity during embryogenesis[16].

We present evidence that Par-6 plays a critical role in the ability of ephrinB1 to regulate TJ formation. Par-6 is a major scaffolding protein that constitutively binds atypical protein kinase C (aPKC) through its PB1 (Phox and Bem 1) domain, and upon binding an active Cdc42-GTP undergoes a conformational change, leading to aPKC activation[17]. The localized activity of the Par-6/aPKC/Cdc42-GTP complex to the apical cell junctions regulates TJ formation, and TJ complexes are believed to associate with the actin cytoskeleton, which is reorganized for the formation and maintenance of cell-cell contacts[18].

Correspondence should be addressed to I.O.D., **Ira O. Daar**, Laboratory of Cell and Developmental Signaling, National Cancer Institute-Frederick, Frederick, Maryland 21702, USA, Tel: 301-846-1667, Fax: 301-846-1666, E-mail: daar@ncifcrf.gov.
[2]Current address: Department of Oncology, Lombardi Comprehensive Cancer Center, Georgetown University Medical Center, Washington DC 20057, USA

Several lines of evidence suggest that Par-6 may be a candidate mediator of ephrinB1 signaling, including significant overlap between *Par-6* and *ephrinB1* RNA expression during development (data not shown), and overlap in protein localization of exogenously expressed proteins along cell-cell boundaries in epithelial cells of the ectoderm in early gastrulae stage embryos (Fig. 1a, 1b). Moreover, immunoprecipitation (IP) analyses of lysates from *Xenopus* oocytes exogenously expressing ephrinB1 and various individual members of the Par polarity complex, identifies Par-6 as specifically present in IPs of ephrinB1 (Fig. 1c), but not other members of the Par complex (Cdc42, Par-3, or PKCλ; Supplementary Information, Fig. S1a, b). Finally, a bacterially expressed protein consisting of the amino terminal portion of Par-6 (His-Flag-Par-6) is detected in an immune-complex of a bacterial expressed protein consisting of the cytoplasmic domain of ephrinB1 fused to GST (Supplementary Information, Fig. S1c), suggesting the interaction may be direct.

To assess whether endogenous ephrinB1 and Par-6 proteins interact, we conducted an IP analysis of ephrinB1 from lysates of HT29 colon carcinoma cells that express abundant levels of Par-6 and ephrinB1. Par-6 is present in ephrinB1 immune-complexes, and in reciprocal IPs ephrinB1 is found in the Par-6 immune-complexes, but not in the control Myc immune-complexes (Fig. 1d). These data indicate that an *in vivo* interaction exists between ephrinB1 and the Par-6 protein.

Since the preceding experiments indicate that ephrinB1 can interact with Par-6, we sought to identify which region of ephrinB1 is necessary for binding to Par-6. We performed an IP analysis on lysates from oocytes co-expressing wild-type and C-terminal deletion constructs of ephrinB1 along with wild-type Par-6. We found that deletion of 16 amino acids from the C-terminus of ephrinB1 (ephrinB1Δ16) prevents the interaction with Par-6 (Supplementary Information, Fig. S2a). Involvement of a possible cryptic PDZ binding motif (aa 309 – 312) was eliminated by using mutants lacking the known and cryptic PDZ binding motifs *in vivo* and *in vitro* (Supplementary Information, Fig. S2b and S2c).

Both Cdc42-GTP and Par-3 bind to Par-6 through the semi-CRIB-PDZ (semi-Cdc42/Rac interacting binding-Postsynaptic density-95/discs large/zonula occludens-1) domain of Par-6[19, 20]. An IP analysis was performed with ephrinB1 and Par-6 deletion constructs, and only a construct retaining all three functional domains (PB1, semi-CRIB and PDZ) of Par-6 was able to bind ephrinB1 (Supplementary Information, Fig. S2d). These data suggest that the appropriate conformation of Par-6 or additional Par-6 interacting proteins may be necessary for a physical interaction between ephrinB1 and Par-6.

Having established that an interaction between ephrinB1 and Par-6 exists *in vivo* (Fig. 1d), we performed loss-of-function studies in *Xenopus* embryos using antisense morpholino oligonucleotides (MOs) to block the expression of endogenous ephrinB1 or Par-6. We injected both blastomeres of 2-cell stage embryos with ephrinB1MO or Par-6MO. MOs that block translation of the endogenous ephrinB1 cause a redistribution of TJ-associated proteins, Zonula Occluden-1 (ZO-1) and Cingulin, but leave intact the lateral expression of Lethal giant larvae 2 (Lgl2; Fig. 2a). Thus, the localization of these proteins to TJs, as evidenced by immunofluorescence, is dramatically diminished. EphrinB1WT$^{\Delta UTR}$ RNA is resistant to the ephrinB1MO, and when introduced at an appropriate level in embryos is capable of rescuing the expression of wild-type ephrinB1, resulting in the restoration of the proper localization of TJ-associated proteins (Fig. 2b). As expected, similar results are obtained with Par-6MO (Supplementary Information, Fig. S3a, b).

Several proteins affecting scaffold function have similar phenotypes with loss or gain-of-function analyses[13, 21–23] (Supplementary Information, Fig. S3c), and may be due to either preventing the formation of signaling centers or sequestering individual members of a signaling

complex, respectively. Since ephrinB1, like Par-6, acts as a signaling platform with no intrinsic activity of its own, the levels of wild-type and mutant ephrinB1 RNAs must be carefully titrated in all of the ephrinB1MO rescue experiments and ephrinB1 over-expression studies (Supplementary Information, Fig. S8a). Thus, we tested whether over-expression of ephrinB1 affects TJ formation in early embryonic ectoderm. Interestingly, the injection of ephrinB1 RNA at levels above those required to replace endogenous ephrinB1 in our rescue experiments also results in disruption of ZO-1 localization at the TJs in early embryonic epithelial cells (Fig. 2c), however, localization of Lgl2 is unaffected (Supplementary Information, Fig. S3d). Transmission electron microscopy (TEM) and dye permeability assays on embryos injected with ephrinB1MO or over-expressing ephrinB1 confirm the structural and functional loss of TJs (Fig. 2d, e, respectively). As expected, more toluidine blue dye permeates the animal pole ectodermal layer of MO-injected and ephrinB1 over-expressing embryos, indicating that TJs and cell-cell junctions are functionally compromised (Fig. 2e). Moreover, even though the localization of TJ-associated proteins is altered, their expression levels remain constant in the presence of ephrinB1MO or ephrinB1 over-expression, and similar results are observed for the Par-6MO and Par-6 over-expression (Supplementary Information, Fig. S3e). These findings demonstrate that the endogenous ephrinB1 is critical for maintaining appropriate localization of TJ-associated proteins and that over-expression of ephrinB1 can influence TJs by re-localizing these proteins and disrupting cell-cell boundaries.

One intriguing possibility of how ephrinB1 may normally regulate TJs is by its interaction with the Par polarity complex, and when inappropriately expressed, ephrinB1 may compete with other member(s) of the complex (Par-3, active Cdc42, or aPKC) for the opportunity to interact with Par-6. To test this concept, we injected RNAs encoding other known members of the Par complex along with ephrinB1 and Par-6, and assessed whether expression of these proteins affected the ephrinB1/Par-6 interaction by examining IPs of Par-6. Interestingly, constitutively active Cdc42 (CA Cdc42) competes with ephrinB1 for binding to Par-6. In Fig. 3a, as increasing amounts of CA Cdc42 are expressed in *Xenopus* oocytes, decreasing amounts of ephrinB1 are found associated with Par-6 in immune-complexes. To confirm this result, we performed a reciprocal experiment, maintaining constant levels of expression of Par-6 and CA Cdc42, but increasing the amount of ephrinB1 expression. In this case, increasing amounts of ephrinB1 were observed in Par-6 IPs, while the amount of CA Cdc42 in the immune-complex correspondingly diminished (Fig. 3a). No such competition is observed with increasing amounts of Par-3 or PKCλ in Par-6 immune-complexes (Supplementary Information, Fig. S4). These results indicate that ephrinB1 and active Cdc42 compete for an interaction with Par-6, suggesting that this may be one of the mechanisms used by ephrinB1 to disrupt TJs.

One prediction of the ephrinB1/Cdc42-GTP competition model is that the disruption of TJs observed with ephrinB1 over-expression *in vivo* (Fig. 2c, d, e; Supplementary Information Fig. S9a) may be rescued by compensatory expression of active Cdc42. In *Xenopus* embryonic ectoderm, appropriate expression of CA Cdc42 rescues TJ localization of ZO-1 that was disrupted as result of ephrinB1 expression (Fig. 3b). In contrast, an inactive Cdc42 (DN Cdc42; which cannot bind to Par-6) fails to rescue ZO-1 localization to TJs (Fig. 3b; Supplementary Information, Fig. S8b, c).

We tested whether the competition model may also play a role in the loss of cell-cell adhesion. It has been previously reported that over-expression of ephrinB1 leads to a visible cell dissociation phenotype in the embryonic ectoderm[10, 11], and we found that over-expression of Par-6 yields a similar phenotype (Supplementary Information, Fig. S5). Expression of CA Cdc42 blocks Par-6-induced cell dissociation, consistent with a role for the active Par-6/Par-3/aPKC/Cdc42-GTP complex in maintaining cell-cell adhesion. In contrast, over-expressing either ephrinB1WT or ephrinB1Δ15 that retains the ability to bind Par-6 can markedly inhibit the rescue of cell-cell adhesion by CA Cdc42, while ephrinB1Δ16 fails to do so (Supplementary

Information, Fig. S5). Collectively, these *in vivo* data support the biochemical analysis indicating that ephrinB1 and active Cdc42 compete for binding to Par-6, and represents a mechanism by which ephrinB1 can influence TJs and cell-cell adhesion.

EphrinB1 can be tyrosine phosphorylated in response to binding a cognate Eph receptor[24, 25] or the TJ-associated protein Claudin[26], or in response to FGF receptor activation[10]. When an active FGF receptor 1 (FGFR1 KE) is expressed in *Xenopus* embryos, phosphorylated ephrinB1 localization is enriched at the apical cell junction, as evidenced by immunofluorescence using phospho-specific antibodies (Fig. 4a). Interestingly, IP and Western analysis of ephrinB1 indicates that phosphorylated ephrinB1 fails to interact with Par-6 (Fig. 4b). Support for this concept is also found in Fig. 3a, where FGFR1 KE is co-expressed along with ephrinB1, Par-6, and CA Cdc42, thus restoring the interaction between CA Cdc42 and Par-6 in IPs (Fig. 3a - last lane). Together, these data indicate that FGF receptor-induced phosphorylation can block the interaction between ephrinB1 and Par-6, and may regulate this interaction at TJs (Supplementary Information Fig. S9a).

Since ephrinB1 is known to be tyrosine phosphorylated upon binding to the ectodomain of its cognate Eph receptor, we tested whether this event also led to the disruption of an association between ephrinB1 and Par-6. Co-IP analysis of endogenous ephrinB1 or Par-6 in HT29 cells in the presence of the EphB1 ectodomain fused to human Fc (EphB1-Fc) demonstrated a clear reduction in the ephrinB1/Par-6 association (Supplementary Information, Fig. S6a). Similar results were found with exogenously expressed proteins in embryo extracts that also exogenously express the cognate EphB1 receptor lacking a kinase domain [EphB1(ΔC); Supplementary Information, Fig. S6b].

To determine which specific tyrosines within ephrinB1 are important for the phosphorylation-dependent dissociation of the ephrinB1/Par-6 complex, several mutants harboring substitutions of Phe for Tyr in the intracellular domain of ephrinB1 were generated, co-expressed with Par-6 and FGFR1 KE, and tested in Co-IPs. An ephrinB1 mutant for tyrosine 310 (ephrinB1Y310F) did not dissociate from Par-6 in the presence of FGFR1 KE (Fig. 4c), indicating that phosphorylation of ephrinB1 on tyrosine 310 prevents or disrupts an interaction between ephrinB1 and Par-6.

We tested whether this tyrosine phosphorylation event regulates the ability of ephrinB1 to influence TJ-associated proteins *in vivo*. As expected, overexpression of ephrinB1 results in the loss of TJ localized expression of ZO-1 (Fig. 5a). This phenotype was unaffected by FGFR1 KD, but was rescued by FGFR1 KE (Fig. 5a), and by co-expression of the truncated cognate receptor EphB1(ΔC) (Supplementary Information, Fig. S6c). Interestingly, a substantial portion of ephrinB1 phosphorylated in response to these proteins is enriched in the TJs (Supplementary Information, Fig. S6c, d). Furthermore, in Fig. 5a, FGFR1 KE failed to rescue the appropriate localization of ZO-1 to TJs when the ephrinB1Y310F mutant was expressed in ectoderm. Together, the *in vivo* and physical interaction data indicate that phosphorylation on tyrosine 310 regulates TJ formation by dissociating ephrinB1 from Par-6.

As further *in vivo* evidence for a role of tyrosine 310 in the dissociation of the ephrinB1/Par-6 complex, we performed ephrinB1 replacement experiments. In these studies, translation of endogenous ephrinB1 is blocked by the ephrinB1MO, and wild-type or mutant ephrinB1 RNAs (ie. ephrinB1WT$^{\Delta UTR}$ or ephrinB1Y310F$^{\Delta UTR}$) that are resistant to the MO are introduced at carefully titrated concentrations. Both of these proteins are expressed at levels that allow ephrinB1WT to rescue the localization of TJ-associated protein ZO-1 in the presence of the ephrinB1MO (Fig. 5b; Supplementary Information, Fig. S8a). In contrast, expression of the ephrinB1Y310F mutant in the presence of ephrinB1MO fails to restore appropriate localization of the TJ-associated protein ZO-1 (Fig. 5b). These data indicate that a tyrosine at position 310

in ephrinB1 is necessary for the proper maintenance of TJs, and is consistent with a phosphorylation event at this position resulting in the dissociation of the ephrinB1/Par-6 complex.

From all these data one may predict that over-expression of ephrinB1 in the embryonic ectoderm, which leads to disruption of the Cdc42-GTP/Par-6 interaction, would result in a reduction of aPKC activity, while phosphorylation of ephrinB1 may rescue this activity. In deed, over-expression of ephrinB1WT causes a marked reduction in aPKC activity towards a Par-3 substrate as well as a decrease in the associated phosphorylation of aPKC. In contrast, the presence of FGFR1 KE or EphB1(ΔC) rescues the aPKC activity (Supplementary Information, Fig. S7a), indicating that phosphorylation of ephrinB1 is critical for aPKC activation and proper functioning of the Par polarity complex at TJs. As expected, loss of endogenous ephrinB1, which results in disruption of TJs, also shows reduced aPKC activity, as evidenced by phospho-aPKC Western analysis (Supplementary Information, Fig. S7b).

Another prediction from this model is that phosphorylation on tyrosine 310 of ephrinB1 may be necessary for the rescue of aPKC activity by FGFR1 KE. The presence of FGFR1 KE rescues aPKC activity that was reduced by ephrinB1 over-expression, but not in the case of the ephrinB1Y310F mutant (Fig. 5c). This data indicates that phosphorylation of ephrinB1 on tyrosine 310 is critical for aPKC activation and proper functioning of the Par polarity complex at TJs. Collectively, our data demonstrate that ephrinB1-induced displacement of active Cdc42 from Par-6 can cause the disruption of TJs, but tyrosine phosphorylation of the intracellular domain of ephrinB1 inhibits the ephrinB1/Par-6 interaction, which results in the proper establishment of TJs (Supplementary Information Fig. S9a, b).

There is compelling evidence that Eph/ephrin signaling plays a critical role in the control of cell-cell adhesion complexes[5, 9, 27] and morphogenetic processes that rely upon the orderly formation of apical junctional complexes. De-regulation of this system in adult tissues can lead to malignant invasion and metastasis. A recent report shows that EphB receptors compartmentalize the expansion of colorectal cancer cells (CRCs) through cell-cell adhesion mechanisms, and this restricts the spreading of EphB-expressing tumor cells into ephrin-B1-positive territories *in vitro* and *in vivo*[28]. This restriction of invasion is dependent upon forward signaling through the EphB receptor[28]. Our study complements this concept by raising the possibility that when ephrinB1 is de-regulated or unphosphorylated in surrounding cells, TJs and cell-cell boundaries are compromised and allow invasion of tumor cells into this adjacent territory. Indeed, loss of EphB receptors has been reported in CRCs[28], consistent with the possible localized loss of Eph receptor-induced ephrinB1 phosphorylation.

Here we present data that ephrin plays a role in TJ integrity and can regulate TJs through the Par complex. A question remains as to whether loss of ephrinB1 results in TJ disruption due to increased availability of Par-6, which then forms non-functional TJ complexes, similar to over-expression of Par-6[29, 30] (Supplementary Information, Fig. S3 and S9c). Alternatively, it is possible that the loss of ephrinB1 may disrupt the appropriate localization of the site of TJ formation, or that disruption of the interaction between ephrinB1 and Connexin43 at gap and adherens junctions[15] disrupts cell adhesion and affects TJs. Understanding how ephrin's role in polarity complexes and adhesion complexes are coordinated to control cell-cell adhesion and boundaries is likely to have implications in morphogenetic disorders and metastatic disease.

Methods

Plasmids and Reagents

A cDNA clone encoding full-length Par-6, Par-3 and PKCλ were obtained from ATCC (GenBank ID: BC073237, NM001092545 and NM001090599). The ephrinB1MO was described previously[31]. The Par-6MO was 25-nucletides long with the respective base composition 5'-GGACTTACTAAAGCTGCGGTTCATC-3' (Gene Tools, Philomath, OR). Various HA-tagged mutants of ephrinB1 (Y310F, V312A, Δ4, Δ4V312A, Δ15, Δ16, Δ17, Δ18 and Δ19) and HA-tagged deletion mutants of Par-6 (PB1, PDZ, CRIB-PDZ, PB1-CRIB-PDZ and C-ter) were generated by PCR, and subcloned into pCS2+. To determine whether tyrosine phosphorylation affects the ephrinB1/Par-6 association, FGFR1 KE (FGFR1 K562E), FGFR1 KD (FGFR1 C289R/K420A) and EphB1 (ΔC)-Flag (aa 1 - 675) constructs in pCS2+ were used.

Embryo Injections

Xenopus embryos were obtained by standard methods[32]. For injections, synthetic capped mRNAs were made using the SP6 mMessage mMachine kit (Ambion, Austin, TX), and microinjected into embryos as previously described[10]. For the rescue of MO effects, MO resistant mRNAs representing ephrinB1ΔUTR, and 4MT Par-6, which either lack the 5' UTR or contain 4 point mutations in wobble codons following the ATG start, were synthesized. MOs and/or mRNAs were microinjected into each blastomere of 2-cell stage embryos.

Immunoprecipitation and Western Blot Analysis

EphB1-Fc (R & D Systems, Minneapolis, MN) was clustered using human Ig as described[33] and added to the HT 29 cells culture medium at a concentration of 2.5 g/ml for 30 min. HT 29 cells, oocytes, embryos or ectodermal explants were prepared with ice-cold lysis buffer as previously described[10]. Immunoprecipitations were conducted for 1 hour on HT 29 cell extracts or 15 oocytes (embryos) equivalents with antibody raised against HA (Applied Biological Materials, Vancouver, Canada), Flag (Applied Biological Materials, Vancouver, Canada), ephrinB1 (Santa Cruz Biotechnology, Santa Cruz, CA) and Par-6 (Santa Cruz Biotechnology, Santa Cruz, CA) and protein-A/G agarose (Santa Cruz Biotechnology, Santa Cruz, CA). Washes and immunoblots were performed as previously described[10] using anti-Flag-HRP conjugated (Sigma, St. Louis, MO), anti-HA-HRP conjugated (Roche, Indianapolis, IN), anti-phosphotyrosine-HRP conjugated (Upstate Biotechnology, Billerica, MA), anti-ephrinB1 (R&D Systems, Minneapolis, MN), or anti-Par-6 (Santa Cruz Biotechnology, Santa Cruz, CA) antibodies. Lysates of ectodermal explants were immunoblotted with anti-phospho-aPKC (Cell Signaling Technology, Danvers, MA), anti-aPKC (Santa Cruz Biotechnology, Santa Cruz, CA), anti-ZO-1 (Invitrogen, Carlsbad, CA), anti-Cingulin (Invitrogen, Carlsbad, CA), and anti-ERK2 (Santa Cruz Biotechnology, Santa Cruz, CA) antibodies.

Immunofluorescence

Xenopus embryos were collected at stage 10.5 and immunofluorescence was carried out as previously described[34]. The following primary antibodies were used: anti-ZO-1 (Invitrogen, Carlsbad, CA; 1/400), anti-Cingulin (Invitrogen, Carlsbad, CA; 1/400), anti-Lgl2 (1/200), and anti-ephrinB1 (Santa Cruz Biotechnology, Santa Cruz, CA; 1/200). Sections were double-stained with a monoclonal anti-HA or anti-Flag antibodies (Applied Biological Materials, Vancouver, Canada; 1/400) to identify ephrinB1-expressing cells, and visualized with fluorescein isothiocyanate (FITC)-conjugated anti-mouse (Invitrogen, Carlsbad, CA; 1/400) or Cy3-conjugated anti-rabbit (Jackson Immuno Research Laboratories, West Grove, PA; 1/400) secondary antibodies on a Zeiss Axioplan fluorescence microscope.

Transmission Electron Microscopy (TEM)

Xenopus embryos were collected at Stage 10.5 and fixed in 4% formaldehyde and 2% glutaraldehyde in 0.1 M cacodylate buffer and processed for thin-section EM analysis. Briefly, the embryos are washed in the same buffer and post fixed in osmium tetroxide (1% in same buffer) for 1 hour. The embryos were washed in cacodylate buffer and in acetate buffer (0.1 M, pH 4.2). The embryos were *en bloc* stained in 0.1% uranyl acetate for 1 hour and dehydrated in a series of ethanol (e.g., 35, 50, 75, 95 and 100%) followed by 3 changes in propylene oxide. The embryos were infiltrated in an equal volume of propylene oxide and epoxy resin overnight and embedded in a pure resin and cured at 55°C for 48 hours. Embryos in the proper orientation were thin-sectioned at 75 nm, mounted on a copper meshed grid, stained in uranyl acetate and lead citrate prior to the EM examination. The digital images were taken on the H7600 microscope equipped an AMT camera.

Dye Permeability Assay

Xenopus embryos were collected at Stage 9.5 and 10.5 and dehydrated in 25, 50, 75, and 100% methanol series. Embryos were then rehydrated by reversing the same methanol series, 1X PBS, and stained with 0.01% toluidine blue (Sigma, St. Louis, MO) for 7 min as described[35].

In vitro Kinase Assays for aPKC

Xenopus ectodermal explants were harvested at Stage 10.5 and prepared with ice-cold lysis buffer as previously described[10]. aPKC IPs were washed with ice-cold lysis buffer and kinase buffer [50 mM Tris-Cl (pH 7.4), 10 mM $MgCl_2$, 1 mM DTT]. 10 μl of samples were used for immunoblots using anti-phospho-aPKC antibody (Cell Signaling Technology, Danvers, MA), and the remaining sample was incubated with 5 μg of GST-Par-3 (aa 688 - 973) in kinase buffer containing 10 μCi of [γ-^{32}P] ATP at 30°C for 30 min. The reactions were stopped by adding 1X SDS/PAGE sample buffer and heating to 100°C. The reaction products were resolved using SDS polyacrylamide (10%) gels and subsequently stained, destained, and dried before autoradiography.

In vitro Binding Assays

Bacterially purified GST-ephrinB1-cyto or *in vitro* translated ephrinB1 (cytoplasmic domain) were incubated with the same amount of purified His-Flag-Par-6 in 750 μl of binding buffer [20 mM Tris-Cl (pH 8.0), 200 mM NaCl, 10 mM Protease inhibitor cocktail] at 4°C for 2 hr. IPs were conducted for 1 hour with antibody raised against GST (Santa Cruz Biotechnology, Santa Cruz, CA). Washes and immunoblots were performed as previously described[10] using anti-Flag-HRP conjugated (Sigma, St. Louis, MO), anti-GST (Santa Cruz Biotechnology, Santa Cruz, CA) antibodies.

Supplementary Material

Refer to Web version on PubMed Central for supplementary material.

ACKNOWLEDGEMENTS

We thank S.Y. Sokol, O. Ossipova and K. Itoh for the Lgl2 antibody, helpful suggestions, and critical reading of this manuscript, K. Nagashima and A. Kamata for TEM, A. Traweger, for GST-Par3 construct, S. Shyam and J. Archaya for critical reading of this manuscript. "This research was supported by the Intramural Research Program of the NIH, National Cancer Institute."

REFERENCES

1. Davy A, Aubin J, Soriano P. Ephrin-B1 forward and reverse signaling are required during mouse development. Genes Dev 2004;18:572–583. [PubMed: 15037550]
2. Cortina C, et al. EphB-ephrin-B interactions suppress colorectal cancer progression by compartmentalizing tumor cells. Nat Genet 2007;39:1376–1383. [PubMed: 17906625]
3. Heroult M, Schaffner F, Augustin HG. Eph receptor and ephrin ligand-mediated interactions during angiogenesis and tumor progression. Exp Cell Res 2006;312:642–650. [PubMed: 16330025]
4. Zhang J, Hughes S. Role of the ephrin and Eph receptor tyrosine kinase families in angiogenesis and development of the cardiovascular system. J Pathol 2006;208:453–461. [PubMed: 16470907]
5. Wimmer-Kleikamp SH, Lackmann M. Eph-modulated cell morphology, adhesion and motility in carcinogenesis. IUBMB Life 2005;57:421–431. [PubMed: 16012051]
6. Cowan CA, Henkemeyer M. Ephrins in reverse, park and drive. Trends Cell Biol 2002;12:339–346. [PubMed: 12185851]
7. Sawai Y, et al. Expression of ephrin-B1 in hepatocellular carcinoma: possible involvement in neovascularization. J Hepatol 2003;39:991–996. [PubMed: 14642617]
8. Surawska H, Ma PC, Salgia R. The role of ephrins and Eph receptors in cancer. Cytokine Growth Factor Rev 2004;15:419–433. [PubMed: 15561600]
9. Pasquale EB. Eph receptor signalling casts a wide net on cell behaviour. Nat Rev Mol Cell Biol 2005;6:462–475. [PubMed: 15928710]
10. Chong LD, Park EK, Latimer E, Friesel R, Daar IO. Fibroblast growth factor receptor-mediated rescue of x-ephrin B1-induced cell dissociation in Xenopus embryos. Mol Cell Biol 2000;20:724–734. [PubMed: 10611251]
11. Jones TL, et al. Loss of cell adhesion in Xenopus laevis embryos mediated by the cytoplasmic domain of XLerk, an erythropoietin-producing hepatocellular ligand. Proc Natl Acad Sci U S A 1998;95:576–581. [PubMed: 9435234]
12. Lu Q, Sun EE, Klein RS, Flanagan JG. Ephrin-B reverse signaling is mediated by a novel PDZ-RGS protein and selectively inhibits G protein-coupled chemoattraction. Cell 2001;105:69–79. [PubMed: 11301003]
13. Lee HS, et al. Dishevelled mediates ephrinB1 signalling in the eye field through the planar cell polarity pathway. Nat Cell Biol 2006;8:55–63. [PubMed: 16362052]
14. Segura I, Essmann CL, Weinges S, Acker-Palmer A. Grb4 and GIT1 transduce ephrinB reverse signals modulating spine morphogenesis and synapse formation. Nat Neurosci 2007;10:301–310. [PubMed: 17310244]
15. Davy A, Bush JO, Soriano P. Inhibition of gap junction communication at ectopic Eph/ephrin boundaries underlies craniofrontonasal syndrome. PLoS Biol 2006;4:e315. [PubMed: 16968134]
16. Shin K, Fogg VC, Margolis B. Tight junctions and cell polarity. Annu Rev Cell Dev Biol 2006;22:207–235. [PubMed: 16771626]
17. Joberty G, Petersen C, Gao L, Macara IG. The cell-polarity protein Par6 links Par3 and atypical protein kinase C to Cdc42. Nat Cell Biol 2000;2:531–539. [PubMed: 10934474]
18. Wang Q, Margolis B. Apical junctional complexes and cell polarity. Kidney Int. 2007
19. Yamanaka T, et al. PAR-6 regulates aPKC activity in a novel way and mediates cell-cell contact-induced formation of the epithelial junctional complex. Genes Cells 2001;6:721–731. [PubMed: 11532031]
20. Gao L, Macara IG. Isoforms of the polarity protein par6 have distinct functions. J Biol Chem 2004;279:41557–41562. [PubMed: 15292221]
21. Liu W, et al. mechanism of activation of the Formin protein Daam1. Proc. Natl. Acad. Sci. USA 2008;105:210–215. [PubMed: 18162551]
22. Qiu RG, Abo A, Steven Martin G. A human homolog of the C. elegans polarity determinant Par-6 links Rac and Cdc42 to PKCzeta signaling and cell transformation. Curr Biol 2000;10:697–707. [PubMed: 10873802]
23. Lin D, et al. A mammalian PAR-3-PAR-6 complex implicated in Cdc42/Rac1 and aPKC signalling and cell polarity. Nat Cell Biol 2000;2:540–547. [PubMed: 10934475]

24. Holland SJ, et al. Juxtamembrane tyrosine residues couple the Eph family receptor EphB2/Nuk to specific SH2 domain proteins in neuronal cells. Embo J 1997;16:3877–3888. [PubMed: 9233798]
25. Bruckner K, Pasquale EB, Klein R. Tyrosine phosphorylation of transmembrane ligands for Eph receptors. Science 1997;275:1640–1643. [PubMed: 9054357]
26. Tanaka M, Kamata R, Sakai R. Phosphorylation of ephrin-B1 via the interaction with claudin following cell-cell contact formation. Embo J 2005;24:3700–3711. [PubMed: 16211011]
27. Miao H, et al. Inhibition of integrin-mediated cell adhesion but not directional cell migration requires catalytic activity of EphB3 receptor tyrosine kinase. Role of Rho family small GTPases. J Biol Chem 2005;280:923–932. [PubMed: 15536074]
28. Batlle E, et al. EphB receptor activity suppresses colorectal cancer progression. Nature 2005;435:1126–1130. [PubMed: 15973414]
29. Gao L, Joberty G, Macara IG. Assembly of epithelial tight junctions is negatively regulated by Par6. Curr Biol 2002;12:221–225. [PubMed: 11839275]
30. Hurd TW, et al. Direct interaction of two polarity complexes implicated in epithelial tight junction assembly. Nat Cell Biol 2003;5:137–142. [PubMed: 12545177]
31. Moore KB, Mood K, Daar IO, Moody SA. Morphogenetic movements underlying eye field formation require interactions between the FGF and ephrinB1 signaling pathways. Dev Cell 2004;6:55–67. [PubMed: 14723847]
32. Moody SA. Cell lineage analysis in Xenopus embryos. Methods Mol Biol 2000;135:331–347. [PubMed: 10791329]
33. Bong Y, et al. ephrinB1 signals from the cell surface to the nucleus by recruitment of STAT3. Proc Natl Acad Sci U S A 2007;104:17305–17310. [PubMed: 17954917]
34. Dollar GL, Weber U, Mlodzik M, Sokol SY. Regulation of Lethal giant larvae by Dishevelled. Nature 2005;437:1376–1380. [PubMed: 16251968]
35. Hardman MJ, Sisi P, Banbury DN, Byrne C. Patterned acquisition of skin barrier function during development. Development 1998;125:1541–1552. [PubMed: 9502735]

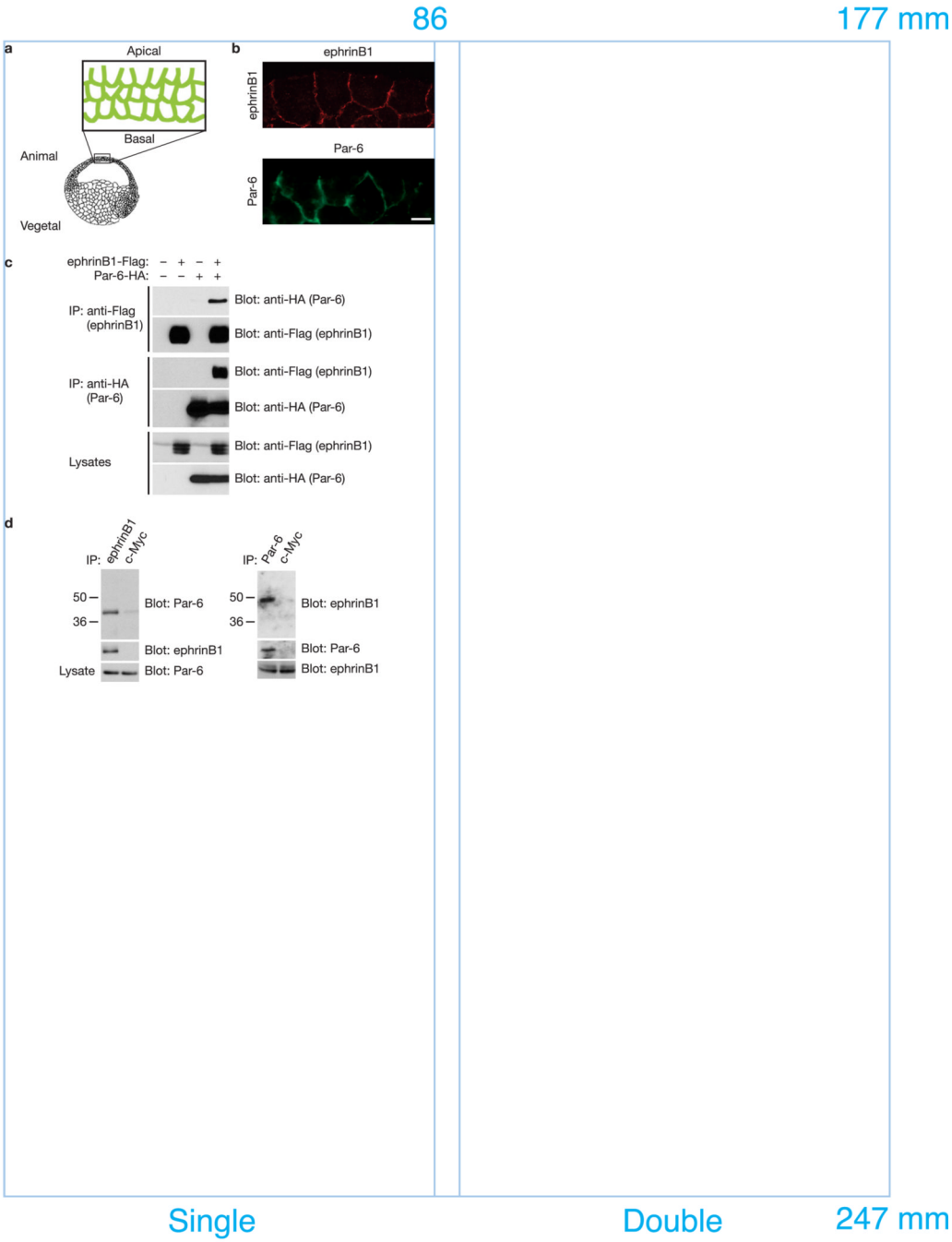

Figure 1. EphrinB1 phrinB1 binds Par-6 *in vivo* and *in vitro*

(**a**) Experimental scheme. Cartoon depicting region of embryo isolated and examined by immunofluorescence. (**b**) Immunofluorescence analysis shows that the localization of ephrinB1 overlaps with that of Par-6 along cell-cell boundaries and the basolateral domain in the gastrula stage (st.10.5) embryos. Each blastomere of 2-cell stage embryos was injected with 100 pg of ephrinB1 or 75 pg of HA-tagged Par-6 RNA where indicated. Embryos were sectioned and immunostained for ephrinB1 (C-18) or Par-6 (HA). The scale bar corresponds to 1 μm. (**c**) Oocytes were left uninjected (−) or injected (+) with Flag-tagged ephrinB1 (10 ng) and HA-tagged Par-6 (10 ng) RNAs where indicated. Oocyte lysates were IP'd with anti-Flag (top and second panels) and anti-HA (third and fourth panels) antibodies, then

immunoblotted with anti-HA or anti-Flag antibodies to detect Par-6 and ephrinB1 proteins. (**d**) Immunoprecipitates using anti-ephrinB1 (rabbit), anti-Par-6 (rabbit) or anti-c-Myc antibodies (rabbit) in HT29 human colon carcinoma cell lysates were immunoblotted with anti-Par-6 (goat) and anti-ephrinB1 antibodies (goat). Lysates were analyzed directly by SDS-PAGE and immunoblotted with indicated antibodies to reveal endogenous expression levels of ephrinB1 and Par-6, respectively.

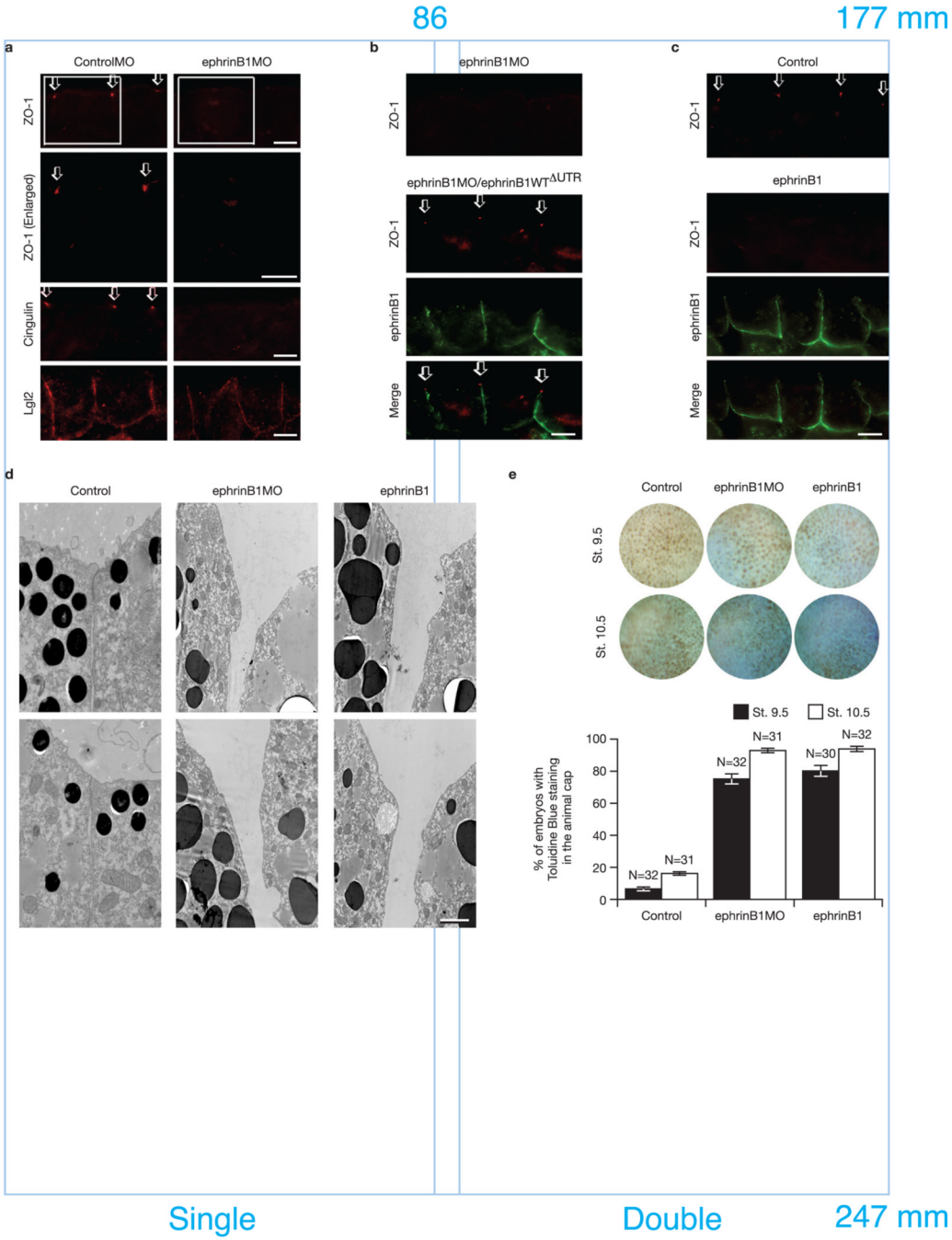

Figure 2. Inhibition and over-expression of ephrinB1 causes the disruption of TJ formation

(**a**) Each blastomere of 2-cell stage embryos was injected with 20 ng of ephrinB1MO or ControlMO where indicated. Embryos were sectioned and immunostained for ZO-1, Cingulin, and Lgl2. Boxed regions of first panel are enlarged in second panel. Arrows indicate the ZO-1 and Cingulin localization in TJs. The scale bar corresponds to 1 μm. (**b**) Each blastomere of 2-cell stage embryos was injected with 20 ng of ephrinB1MO and 150 pg of ephrinB1WT$^{\Delta UTR}$-HA RNA where indicated. ΔUTR indicates use of a mutant RNA lacking a 5' UTR sequence which is complementary to the ephrinB1MO, conferring resistance to the ephrinB1MO. Embryos were sectioned and immunostained for ZO-1 and ephrinB1 (HA). Arrows indicate the ZO-1 localization in TJs. The scale bar corresponds to 1 μm. (**c**) Each

blastomere of 2-cell stage embryos was injected with 200 pg of ephrinB1-HA RNA. Embryos were sectioned and immunostained for ZO-1 and ephrinB1 (HA). Arrows indicate the ZO-1 localization in TJs. The scale bar corresponds to 1 μm. (**d**) Each blastomere of 2-cell stage embryos was injected with 20 ng of ephrinB1MO or 150 pg of ephrinB1-HA RNA and collected at Stage 10.5. Transmission electron microscopy shows disruption of TJs when ephrinB1 is inhibited or over-expressed in embryos. The scale bar corresponds to 0.5 μm. (**e**) Each blastomere of 2-cell stage embryos was injected with 20 ng of ephrinB1MO or 150 pg of ephrinB1-HA RNA. Embryos were collected at stage 9.5 and 10.5 and stained with 0.01% toluidine blue. At each stage, positive stained embryos were counted from each group and presented as a percentage (see histogram). Embryos were scored as positive when over 10% (St. 9.5) or over 50% (St. 10.5) of the ectodermal surface was stained. Note: More toluidine blue dye permeated the animal pole ectodermal layer of MO-injected (75.0±3.13% − 90.4 ±0.74% sem of embryos) and ephrinB1 over-expressing embryos (80.0±1.19% − 93.8±1.56% sem of embryos) than control (6.3±1.56% − 16.3±0.95% sem of embryos).

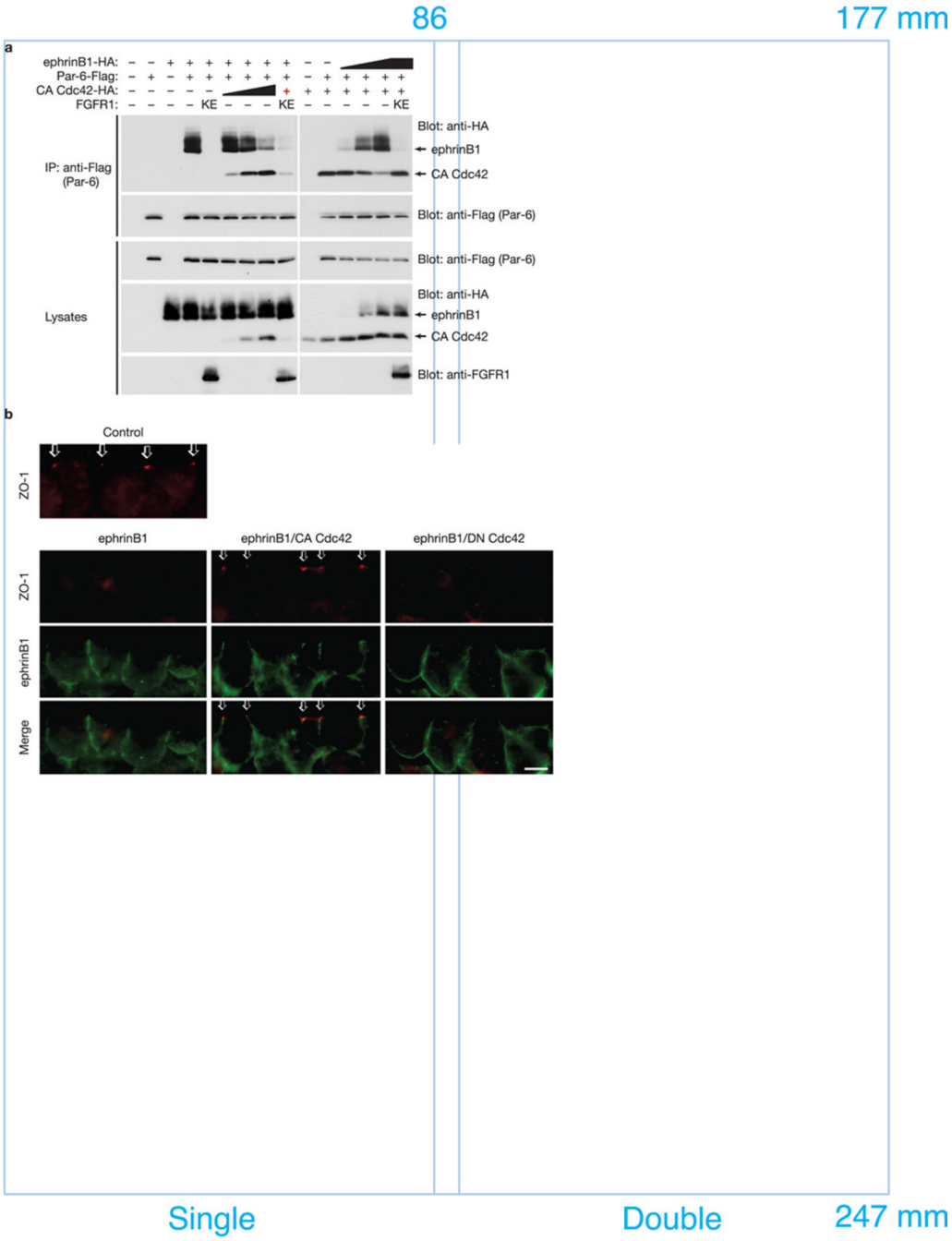

Figure 3. EphrinB1 and active Cdc42 compete for Par-6 binding

(**a**) Oocytes were left uninjected (−) or injected (+) with Par-6-Flag (10 ng) plus ephrinB1-HA (10 ng) and increasing amounts (1, 5, 10 ng) of CA Cdc42-HA RNAs or alternatively with Par-6-Flag (10 ng) plus CA Cdc42-HA (10 ng) and increasing amounts (1, 5, 10 ng) of ephrinB1-HA RNAs as indicated. Oocyte lysates were IP'd with anti-Flag antibody, then immunoblotted with anti-HA antibodies to detect ephrinB1 and active Cdc42 proteins. Oocyte lysates were analyzed directly by SDS-PAGE and immunoblotted with indicated antibodies. Note: the red + indicates the lowest amount of CA Cdc42-HA RNA (1 ng) was used. (**b**) Each blastomere of 2-cell stage embryos was injected with 200 pg of ephrinB1WT-Flag and 50 pg of CA Cdc42-HA or DN Cdc42-HA RNAs where indicated. Embryos were sectioned and

immunostained for ZO-1 and ephrinB1 (Flag). Arrows indicate the ZO-1 localization in TJs. The scale bar corresponds to 1 μm.

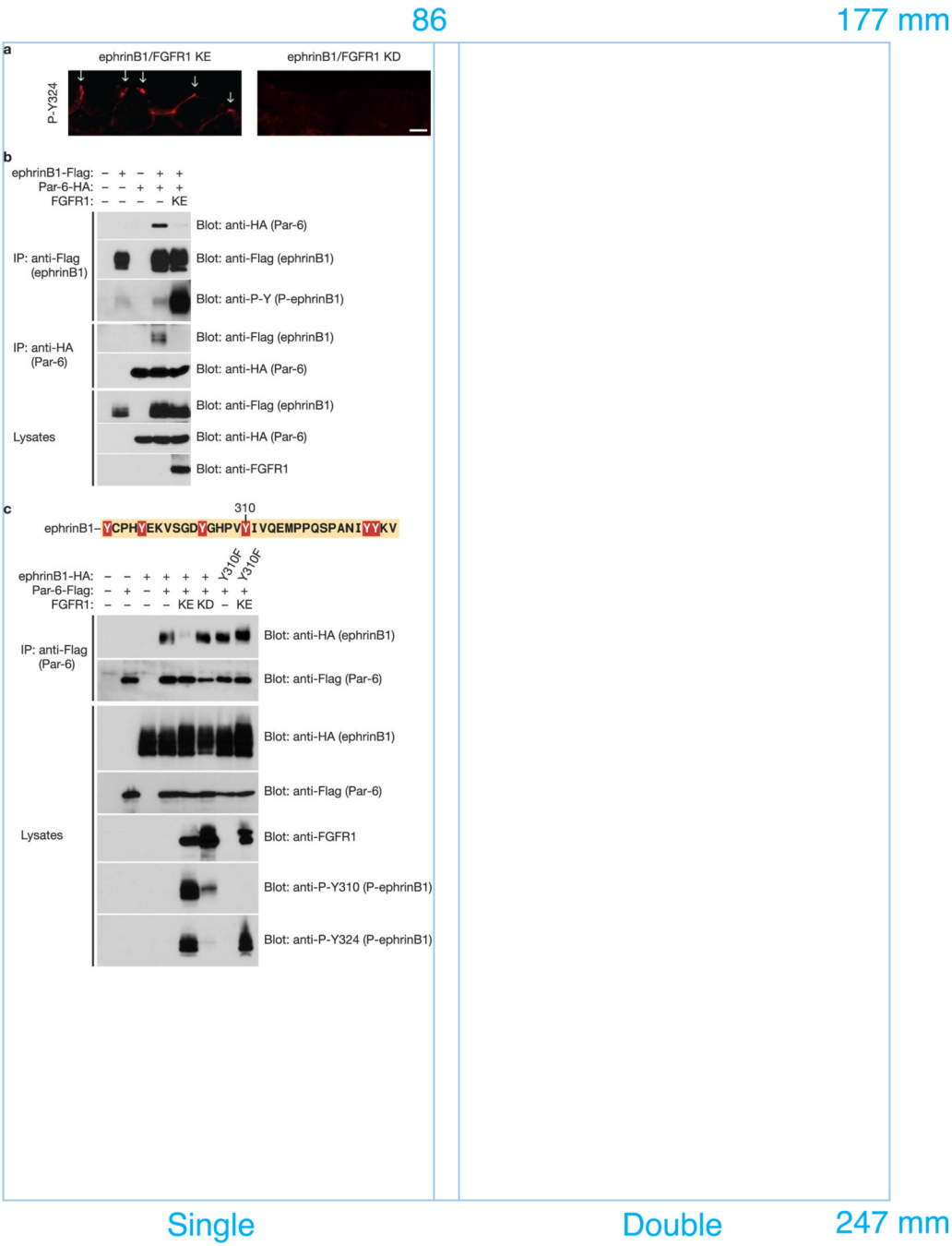

Figure 4. FGF signaling blocks the interaction between ephrinB1 and Par-6 through the tyrosine phosphorylation of the intracellular domain of ephrinB1

(**a**) Each blastomere of 2-cell stage embryos was injected with 200 pg of ephrinB1-HA and 200 pg of FGFR1 KE or FGFR1 KD RNAs where indicated. Embryos were sectioned and immunostained for phosphorylated ephrinB1 (P-Y324). Arrows indicate the presence of phosphorylated ephrinB1 in apical cell junctions. The scale bar corresponds to 1 μm. (**b**) Oocytes were left uninjected (−) or injected (+) with ephrinB1-Flag (10 ng), Par-6-HA (10 ng) and FGFR1 KE (10 ng) RNAs as indicated. Oocyte lysates were IP'd with anti-Flag (top, second, and third panels) or anti-HA (fourth and fifth panels) antibodies, then immunoblotted with either anti-HA or anti-Flag antibodies to detect bound proteins. Oocyte lysates were

analyzed directly by SDS-PAGE and immunoblotted with indicated antibodies. (**c**) Oocytes were left uninjected (−) or injected (+) with ephrinB1WT-HA (10 ng) or ephrinB1Y310F-HA (10 ng), Par-6-Flag (10 ng) and FGFR1 KE (10 ng) or FGFR1 KD (10 ng) RNAs as indicated. Oocyte lysates were IP'd with anti-Flag antibody, then immunoblotted with anti-HA antibody to detect ephrinB1 proteins. Oocyte lysates were analyzed directly by SDS-PAGE and immunoblotted with indicated antibodies.

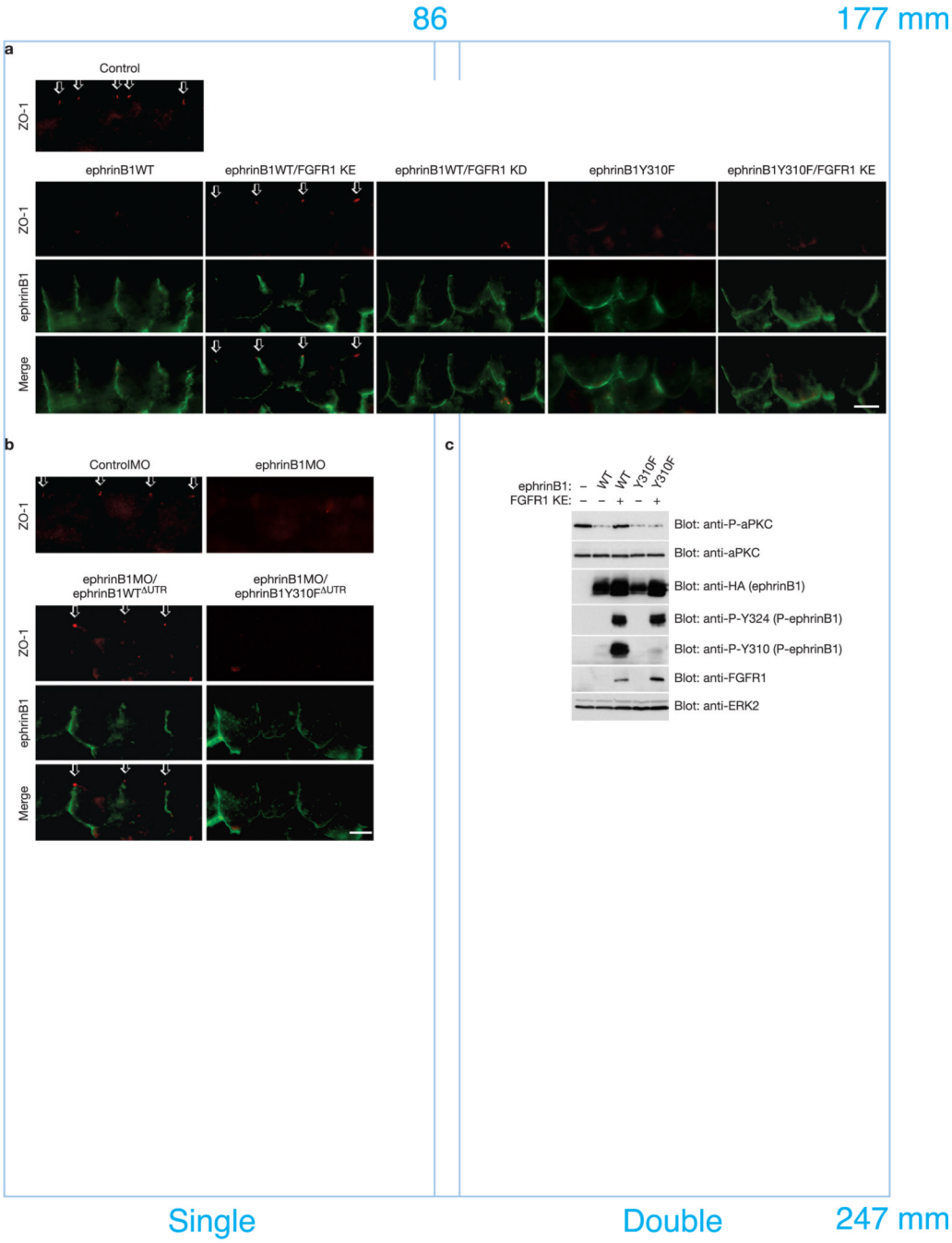

Figure 5. Phosphorylation on tyrosine 310 regulates TJ formation by dissociating ephrinB1 from Par-6

(**a**) Each blastomere of 2-cell stage embryos was injected with 200 pg of ephrinB1WT-HA or ephrinB1Y310F-HA and 200 pg of FGFR1 KE or FGFR1 KD RNAs where indicated. Embryos were sectioned and immunostained for ZO-1 and ephrinB1 (HA). Arrows indicate the ZO-1 localization in TJs. The scale bar corresponds to 1 μm. (**b**) Each blastomere of 2-cell stage embryos was injected with 20 ng of ControlMO or ephrinB1MO and 150 pg of ephrinB1WT$^{\Delta UTR}$-HA or ephrinB1Y310$^{\Delta UTR}$-HA RNAs where indicated. Embryos were sectioned and immunostained for ZO-1 and ephrinB1 (HA). Arrows indicate the ZO-1 localization in TJs. The scale bar corresponds to 1 μm. (**c**) Each blastomere of 2-cell stage

embryos was injected with 200 pg of ephrinB1-HA or ephrinB1Y310-HA and 200 pg of FGFR1 KE RNAs where indicated. At stage 8.5, ectodermal explants were dissected, and harvested at stage 10.5. Lysates of these explants were analyzed directly by SDS-PAGE and immunoblotted with indicated antibodies.